water

MDPI

Article

Impact of Sediment Deposition on Flood Carrying Capacity of an Alluvial Channel: A Case Study of the Lower Indus Basin

Arslan Mahmood [1,2], Jing-Cheng Han [1,*], Muhammad Wajid Ijaz [3], Altaf Ali Siyal [4], Muhammad Ahmad [1] and Maryam Yousaf [1]

[1] Water Science and Environmental Engineering Research Center, College of Chemical and Environmental Engineering, Shenzhen University, Shenzhen 518060, China
[2] Irrigation Department, Government of the Punjab, Lahore 54000, Pakistan
[3] Environment Protection Department, Government of the Punjab, Lahore 54000, Pakistan
[4] Department of Land and Water Management, Sindh Agriculture University, Tandojam 70060, Pakistan
* Correspondence: hanjc@szu.edu.cn; Tel.: +86-18124141306

Abstract: Impacts of climate change and human-made interventions have altered the fluvial regime of most rivers. The increasingly uncertain floods would further threaten the flow delivery system in regions such as Pakistan. In this study, an alluvial reach of the Indus River below Kotri barrage was investigated for the geomorphologic effects of sediments deposited over the floodplain as well as the influences on the downstream flood-carrying capacity. The hydrodynamic modeling suite HEC-RAS in combination with ground and remotely sensed data were used to undertake this analysis. Results suggest that the morphology of the river reach has degraded due to depleted flows over a long period and hydrological extremes that have led to excessive sediment deposition over the floodplain and an enhancement in flood water extension possibility over the banks. A deposition of 4.3 billion cubic meters (BCM) of sediment increased the elevation of the channel bed which in turn reduced a 17.75% flood-carrying capacity of the river reach. Moreover, the excessive deposition of sediments and the persistence of low flows have caused a loss of 48.34% bank-full discharges over the past 24 years. Consequently, the river's active reach has been flattened, with a live threat of left levee failure and the inundation of the populous city of Hyderabad. The study would gain insights into characterizing the impacts associated with a reduction in the flood-carrying capacity of the alluvial channel on account of the inadequate sediment transport capacity after heavy flow regulations.

Keywords: alluvial reach; flood-carrying capacity; flow regulations; hydraulic modeling; Indus river

Citation: Mahmood, A.; Han, J.-C.; Ijaz, M.W.; Siyal, A.A.; Ahmad, M.; Yousaf, M. Impact of Sediment Deposition on Flood Carrying Capacity of an Alluvial Channel: A Case Study of the Lower Indus Basin. *Water* **2022**, *14*, 3321. https://doi.org/10.3390/w14203321

Academic Editor: Ataur Rahman

Received: 23 September 2022
Accepted: 18 October 2022
Published: 20 October 2022

1. Introduction

The 2010 and 2022 floods in the Indus river started from late July to mid-September due to monsoon rains in the upper catchments of the Indus basin. It dragged sediments from the catchment area of the Tarbela dam to the floodplain downstream of the Kotri barrage, and eventually contributed the sediment to the Indus delta. These flood events have contributed to changing the river morphology in terms of excessive sediment deposition on the river floodplain. The sediment layers are reworked at bank-full and regular discharges, deforming the active riverine channels for pattern reconfiguration [1]. Such channels can be termed as morphologically active channels [2] formed by the reworking of sediments over a specific duration of time, i.e., during flood events. A morphologically active channel's magnitude increases at high flows through the horizontal and vertical expansion of channel width and depth [1,3], triggering the reworking of the sediment deposits adjacent to an active channel. This results in channel erosion and the transportation of sediment flux [4], known as the fluvial process, which directly impacts the flood-carrying capacity of the river. The Indus river reaching immediately downstream of the Kotri barrage is a natural physical model to study and interpret the fluvial processes of the Indus river.

Channel erosion, sediment transportation, and deposition are the key factors that control river morphology under given flow patterns [4]. A significant amount of sediment is transported during flood events, which is trapped behind hydraulic structures and human-made constrictions across the flow of the Indus river. The river experienced flow diversions and sediment reduction with the introduction of six barrages (Jinnah, Chashma, Taunsa, Guddu, Sukkur, and Kotri) and he Tarbela dam (3.69 km^3 storage capacity) during 1932–1976. These flow regulations have altered its fluvial regime [5], with the increase in the number of no-flow days [6] and a reduction in the mean annual discharge [7]. This state of affairs has ultimately resulted in the degradation of the river geomorphology [8,9] due to sediment trapping behind the hydraulic structures [8,10,11].

The Indus river transforms into an alluvial river in its lower reaches over the flatter terrain of lower Sindh and ultimately opens into the Arabian Sea [12,13]. It is the 21st largest river in the world in terms of annual flow [14]. However, the constructed or artificially reinforced levees confine the course of the Indus river, and in turn, affect the morphology of the alluvial riverbed. Wang et al. [15] defined an alluvial river as one with erodible boundaries flowing in self-formed channels, such as the morphology of lower reaches of the Yellow River and the middle and lower reaches of the Yangtze River [16]. The Lower Indus Basin also consists of alluvial soils brought from Himalayan ranges and the lower Indus plain [17]. Thus, an alluvial rivers' channel bed, consisting of sand and silt, encounters channel evolution as a response to shifting flow intensity and sediment deposits [15]. Accordingly, the study of alluvial river streams necessitates the assessment of sedimentary planforms and their movement which changes with high/low flows.

Various researchers have investigated the hydrogeomorphology of the Indus and worldwide rivers. For instance, Boota et al. [18] assessed the hydrogeomorphology of the Indus river and iterated the imbalanced dynamic equilibrium resulting in unstable channel cross-sections, with coarser sedimentary particles impacting the riverine morphology during flood episodes. A balanced channel ecosystem necessitates proper sedimentary budget for the morphologic sustainability [19]. Thus, the Indus river flood protection works vitalize the need to study sedimentary dynamics and the fluvial regime so to control the governing factors that assist river migration and avulsion processes. Singh et al. [20] studied the morphological dynamics of the Ganga River in terms of erosion, transportation, and deposition processes of terrigenous clastic sediments transported from the continents to the oceans by rivers. The relations between riverine sediment transport, channel geometry, hydrology, and aggradation of flood plain can define the active channel geometry and migration patterns [20]. Moreover, the increased sediment yields from mountainous rivers in the Himalayan and Tibetan Plateaus are attributed to climate change [21–23].

Similarly, Wang et al. [15] studied the sedimentation rate of the Lower Yellow River and compared changes in the riverbed due to accretion. The increased sedimentation rate has raised the riverbed and floodplains of the Lower Yellow River by 5 m in the past 70 years, forming a perched river and drastically reducing river flow capacity. Thus, the Lower Yellow River experienced 1593 levee breaches from 602 BC to 1949 AD, flooding vast areas and claiming millions of lives. Consequently, the Lower Yellow River was dubbed "the sorrow of China". The Lower Indus Report by WAPDA [17] revealed that the Lower Indus Basin consists of alluvial soils, which lie within the range of fine sandy loam to silty clay. The organic content in the soils is less than one percent and decreases rapidly with depth. Soils are structureless, and the only aggregating agent is calcium carbonate, which has been conveyed with sediments from the Himalayas. That is why the alluvial channel is more prone to morphological vulnerability, especially in the flatter terrain of the Lower Indus Basin. Various studies show that sediment entrapment behind hydraulic structures has lowered the sediment load in the Indus River flows below the Kotri Barrage [10,11]. However, due to the discharge of relatively sediment-free water, the probability of channel erosion has increased due to the enhanced sediment-removing capacity. Meanwhile, the recent major flooding events in the Indus Basin were witnessed in 2010 (24,618 m^3/s peak flow) and 2015 (17,091 m^3/s peak flow) at the Kotri barrage. The deposition of an immense

quantity of sediments over the river floodplains was one of the notable aftermaths of the events. It apparently disturbed the regime of the river, and active channels started deforming their courses in accordance with the new flow regime.

Thus, this study aims to explore the role of sediment deposits over the floodplain of an alluvial river and the consequent effect on the channel's flood-carrying capacity. To achieve this, scenarios of flooding in 1D-unsteady flow model simulations based on HEC-RAS, with and without sediment deposits, are simulated. The specific objectives are: (1) to study the impact of sediment deposition on river hydrogeomorphology using remote sensing and hydraulic modeling techniques, and (2) to optimize the river geometry, idealizing complete sediment removal, for enhancing the flow capacity of the river and reducing flood hazards associated with different flow conditions. The study would be a significant contribution to research literature in terms of preserving the stability of alluvial rivers across the world and assessing the flood hazards associated with the flood-carrying capacity of the river. The findings would help the Irrigation Department, Government of Sindh, to optimize solutions for preserving the river boundaries and the environmental value of the deposited sediment.

2. Materials and Methods

2.1. Study Area

The study area lies in the Lower Indus Plain near Jamshoro, Sindh-Pakistan, and spans between the Kotri barrage to the Bypass bridge. The Kotri Barrage, built in 1955, is the last hydraulic structure erected across the Indus River with a design discharge of 24,777.2 m^3/s ("m^3/s", also denoted by cumecs in this paper). It is situated around 200 km landward from the Arabian Sea and is used to regulate the freshwater supplies to the Indus Delta. Moreover, four major canals (Phuleli, Pinyari, Kalri Baghar Feeder, and Akram Wah) draw water from the barrage for municipal and agricultural uses. Geographically, the study river-reach spans between 25°26′33.50″ N–25°24′11.18″ N and 68°18′57.17″ E–68°18′35.16″ E (Figure 1). The total study area covers 576 hectares, with artificial levees along both sides of the channel. The terrain is flat and the climatology is arid. There are huge sediment deposits over the river floodplain beyond which the right protection bank exists.

2.2. Hydrologic Analysis

Flood peaks and annual discharge (43 years of data) from 1976 (when the largest dam started impoundment across the Indus) to 2018, based on 10-daily values passed from the Kotri Barrage, were collected from the Sindh Irrigation Department. Flood frequency analysis was undertaken using United States Geological Survey (USGS) recommended Index Flood Method [24,25]. For convenience of analysis, 4 decadal slices of timeline were demarked for classification of flood flows according to Indus River System Authority (IRSA).

2.3. Landscape Analysis

The Lower Indus Basin below the Kotri Barrage falls in the alluvial category, and sediment deposition and erosion define its channel planform. The Normalized Difference Water Index (NDWI) was used for the delineation of water extent in the study reach. It was calculated using the ratio of near infrared (NIR) and the green band [26] of multispectral imageries (Equation (1)) captured by Landsat-5 and Landsat-8 from 1990 to 2018. Using high-resolution images would help to implement best management practice [27], and the interpretation of the satellite images was made with ground observations and high-resolution satellite images available in time series of Google Earth, as reported by Ijaz et al. [28]. It enabled to study the active channel migration pattern and adjoining floodplain areas.

$$\text{NDWI} = (\text{Green} - \text{NIR})/(\text{Green} + \text{NIR}) \quad (1)$$

Landsat images with cloud cover of less than 10% from 1990 to 2018 were acquired from the US Geological Survey (USGS), as described in Table 1 below.

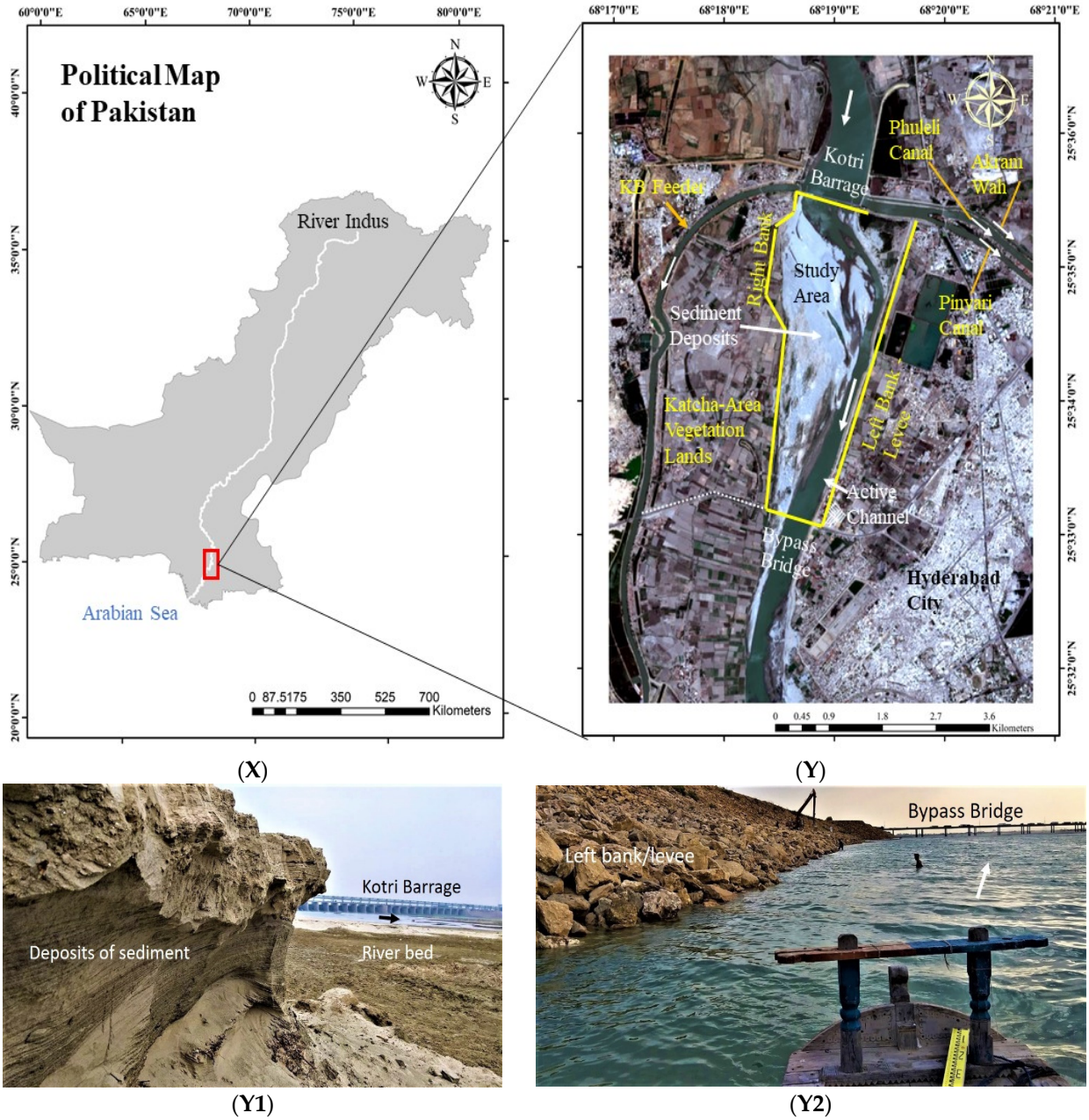

Figure 1. Image (**X**) depicts the location of study area while image (**Y**) is location map of the Indus river-reach spanning from the Kotri Barrage to the Bypass Bridge. The inset closer views of the downstream side of the barrage, i.e., images (**Y1**,**Y2**), demonstrate sedimentary deposit and branches of the active channel. River flow opts either or all channels as per sequential gates operation of the barrage.

Table 1. Detail of satellite imageries processed for detection of surface water extent corresponding to discharge.

Sr. No.	Image Acquired	Sensor	River Flow (m^3/s)	Sr. No.	Image Acquired	Sensor	River Flow (m^3/s)
1	13/09/1990	TM	4123.26	21	29/04/2010	TM	0
2	31/08/1991	TM	3083.24	22	16/06/2010	TM	0
3	17/08/1992	TM	14,081.45	23	02/07/2010	TM	5.66
4	04/08/1993	TM	9340.40	24	19/08/2010	TM	8096.33
5	20/08/1993	TM	4480.33	25	04/09/2010	TM	20,054.80
6	23/08/1994	TM	22,549.71	26	22/10/2010	TM	677.29
7	10/10/1994	TM	1173.21	27	23/11/2010	TM	388.23
8	13/12/1994	TM	0	28	25/12/2010	TM	181.36
9	06/05/1995	TM	835.98	29	26/01/2011	TM	0
0	15/10/1996	TM	136.02	30	11/02/2011	TM	0
11	15/08/1997	TM	1887.35	31	31/30/2011	TM	0
12	12/05/1997	TM	0	32	02/05/2011	TM	0
13	18/08/1998	TM	3944.73	33	03/06/2011	TM	187.03
14	05/08/1999	TM	1825.00	34	05/07/2011	TM	181.36
15	23/08/2000	TM	0	35	22/08/2011	TM	844.49
16	26/08/2001	TM	300.38	36	14/08/2014	OLI	0
17	10/06/2002	TM	0	37	17/08/2015	OLI	16,437.38
18	17/09/2009	TM	70.84	38	19/08/2016	OLI	2673.06
19	23/01/2010	TM	0	39	18/03/2018	OLI	0
20	04/02/2010	TM	0				

Note: TM stands for Thematic Mapper and OLI is Operational Land Imager.

2.4. Hydraulic Analysis

Primary data, including reconnaissance and bathymetric survey of the study reach, channel bed-forms, and land-use, were collected during field visits made in 2017–2018 in collaboration with Sindh Irrigation Department. Inundation extents corresponding to known discharges were derived from the remotely sensed images and used for the assessment of impacts of sediment deposition on flood-carrying capacity of the channel. River Analysis System of the Hydrologic Engineering Center (HEC-RAS 4.1)—a 1D hydraulic model was employed for hydraulic computations. Geometric representation of the study reach was a build-up in HEC-GeoRAS using Digital Surface Model 30 m (https://www.eorc.jaxa.jp/ALOS/en/aw3d30/index.htm) accessed on 1 October 2020. Cross-sectional geometry was corrected in the geometric editor of the suite using data collected during the bathymetric survey by following Tadono et al. [29] and Ijaz et al. [30].

Mean daily discharge values and corresponding reduced water levels collected from the Sindh Irrigation Department for the years 1990–2018 were employed for establishing the upstream boundary conditions. The water marks and corresponding levels observed in the middle and lower sections of the study reach were utilized for calibration and validation of the modelled values.

The cross-section spacing was confirmed using Courant conditions, while a rational time step was selected by satisfying the Courant Number to ensure the numerical accuracy of the intended computations [31]. The Manning's roughness coefficient (n) values were assigned to the main channel, left bank, and right bank at each cross-section. For a logical start, the 'n' value were calculated using Stickler's formula [32]. In addition, Manning's roughness coefficient ranges were considered during the iterative process for model calibration as defined by Brunner [31] for natural streams and Simons et al. [33] for various floodplains and bed-forms. According to recommended procedure, the calibration of the hydraulic model was done in steady flow mode through the comparison of observed and simulated flow hydrograph for the 2010 flood downstream of the Kotri barrage (Figure 1). The validation of computed water levels corresponding to assigned discharge was made using measured height of watermarks noticeable on the left bank.

3. Results and Discussion

3.1. Hydrologic Analysis

Water flows from the Kotri Barrage do not follow a uniform pattern of releases. The annual average flood peaks and escapage downstream of the barrage from 1976 to 2018 have witnessed a noticeable decrease of 40.1% and 67%, respectively (Figure 2). The magnitude of annual flows has diminished for the past 44 years based on the linear trend, with a minimum of 2 billion cubic meters (BCM) annual escape in the year 2018. There is a distinct difference between the annual peak flow and annual escapage before and after year 2000. Before the year 2000, the annual escapage with respect to the flood peak was greater. However, after the year 2000, flow records revealed that annual discharges had been diminished, but the flood peaks were sharp.

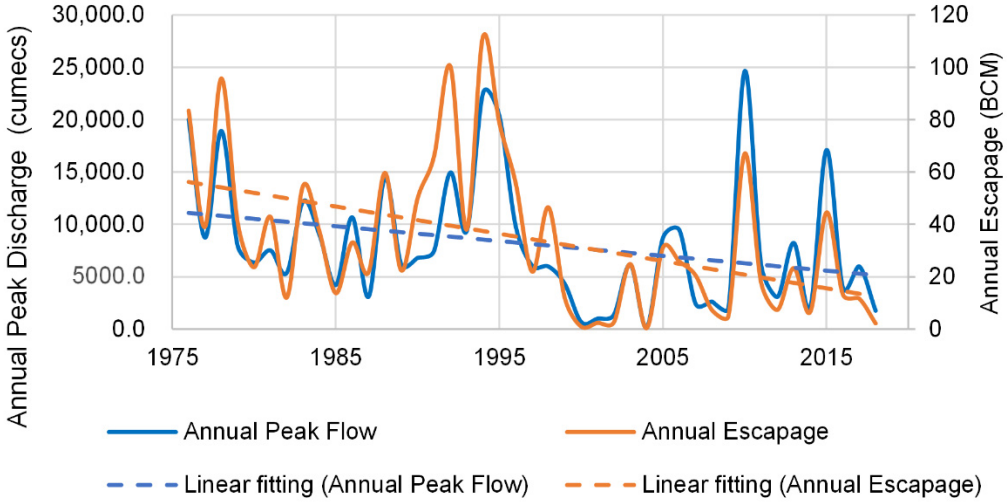

Figure 2. Temporal variation of annual peak discharge and annual escapage downstream of the Kotri barrage from 1976 to 2018.

The Indus River System Authority (IRSA) classifies the flood peaks into five major classes as low, medium, high, very high, and exceptionally high flood events (Table 2). The frequency analysis revealed that low flood flows and exceptionally high floods from 1976 to 2018 were 60% and 9%, respectively. It confirms that high-flow regulations have significantly altered the fluvial regime of the Indus River. This significant change in fluvial flows warrants a thorough investigation of the hydromorphology of the reach to ascertain response of the channel and the adjacent floodplain.

Table 2. Categorized flood peaks occurrence and water escape pattern below the Kotri barrage.

Hydrologic Years	Low	Medium	High	Very High	Exceptionally High	Average Annual Peak (1000 m^3/s)	Average Volume Released (BCM)
	Flow Velocity (1000 m^3/s)						
	8.5	9.9	14.2	19.8	25.5		
	Return Period (years)						
	1.4	1.8	4.1	11.5	33.2		
	Frequency analysis						
1976–1985	04	02	01	01	01	10.01	44.27
1986–1995	04	01	01	02	02	11.57	58.14
1996–2005	08	02	00	00	00	4.42	19.81
2006–2018	10	01	00	01	01	6.86	19.38

3.2. Landscape Analysis

NDWI was used to analyze the spatiotemporal variability of the alluvial channel and adjoining riverine area through extraction of planimetric characteristics of the reach. Figure 3 depicts the total area of the active river-reach as 576 hectares. The proportions of water and non-water pixels distinguished from the images of the years 2010 and 2015 were markedly different from the other years. Visual inspection and ground-truthing surveys confirm that exceptionally high floods caused overtopping of the right bank and inundated 1141 hectares in 2010 and 1134 hectares in 2015, respectively (Figure 4). The total area covered with sediments shows a positive linear trend over the period from 1990 to 2018, which is an indication of an increase in sediment deposits in the study reach. Moreover, the area inundated outside the active river reach is referred as the Katcha area (locally used for floodplain) and is usually cultivated.

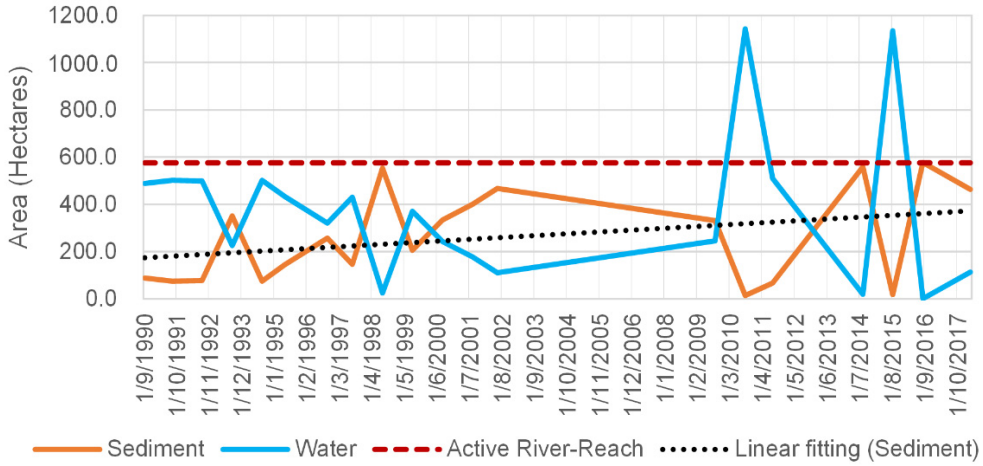

Figure 3. NDWI analysis of the study river-reach using Band 2 (Green) and Band 4 (NIR) of Landsat imagery from 1990 to 2018.

Figure 4a exhibits the presence of three active channels (left, middle, and right) in December 1994 after the passage of an exceptionally high flood (22,550 m^3/s) in August 1994. However, another exceptionally high flood (20,330 m^3/s) passed downstream of the Kotri Barrage in 1995 (Table 2), which resulted in alteration in the morphology of the active river-reach through the deposition of sediments along the right and middle reach (Figure 4b). The river started flowing from the narrow right and wide left active branches. In Figure 4c, only one channel can be seen active at a negligible discharge. This channel switching was witnessed after an exceptionally high flood passed in 2010 (Table 2), which has deposited and reworked the bed-load sediment over the riverine floodplain and the fluvial morphology of the river adopted to the new flow regime.

The sediment deposits on the right side of the river reach accreted continuously in the wake of floods passed in 1994, 1995, 2010, and 2015. This resulted in the plugging of the right and central branch channels, and the only left channel adjacent to the left bank remained active, as depicted in Figure 4d. Gate operations of the barrage, along with the sediment deposition pattern over the floodplain, considerably changed the hydromorphology of study reach. Ashmore et al. [1] defines such a channel as a morphologically active channel in which bed-load transport occurs over short periods and the river behaves in an unstable manner, as in the case of the current study. It is worthy to consider that the only active channel has overridden the artificially reinforced left levee. The persistence of the flow routing through the left active channel poses the threat of levee breach and the subsequent urban flooding in adjoining areas, i.e., Hyderabad city.

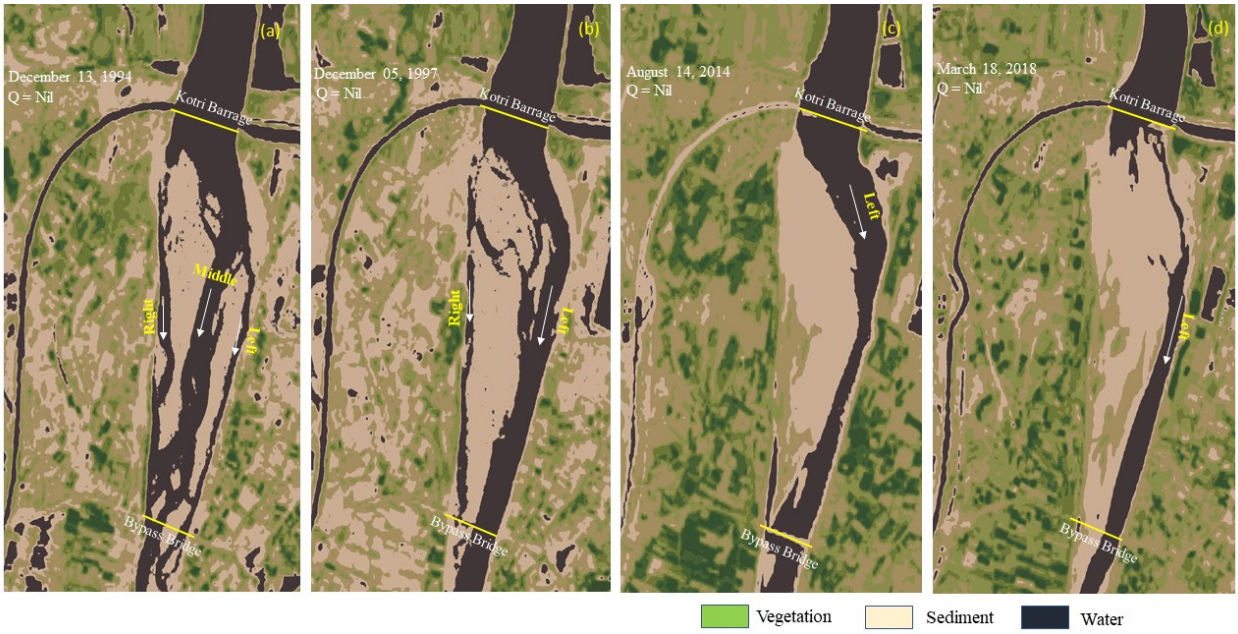

Figure 4. Visual comparisons of Landsat imageries for the study area river-reach. (**a**) TM acquired an image on 13 December 1994, showing three active riverine channels at zero discharge; (**b**) TM acquired an image on 5 December 1997, showing two active riverine channels at zero discharge; (**c**) OLI and TIRS acquired an image on 14 August 2014, resulting in only one active riverine channel at zero discharge; (**d**) OLI and TIRS acquired an image on 18 March 2018, representing only one active riverine channel at zero discharge.

The impact of sediment deposits is understandable from Figure 5a, which reveals that an exceptionally high flood (22,550 m^3/s) passed safely through the riverine channels during the year 1994, as there were three sufficient active channels. However, during 2010, the active river channels could not successfully pass the peak flow (20,055 m^3/s). Consequently, the flood water overtopped the right bank and inundated 565 hectares of the Katcha area (Figure 5b). This pattern of riverine behavior constitutes that sediment deposits play a key role in the flood-carrying capacity of an alluvial reach. Another event of identical nature was witnessed during the 2015 flood, when the morphologically active riverine channel failed to stream the high flood (16,437 m^3/s) downstream and overflowed 558 hectares of the Katcha area (Figure 5c).

The nature of the bed-load transport is braiding as the volume of sediment was reworked during short flood events, where the bank-full discharge resulted in channel pattern reconfiguration from right to left. The reduced bed material mobility, pertaining to low flows during 2000–2009, and low to medium flows during 2011–2014 (Figure 2), impacted the morphologic characteristics of the alluvial riverbed, which adjusts itself to the new flow regime. This new regime inherits the sediment heaps that more likely impact the flood-carrying capacity of the channel.

Apparently, the aggradation of riverbed on the right side of fluvial floodplain would bring about the flooding of the area twice the size of the active river reach during 2010 and 2015 floods (Figure 6). However, the flood intensity was different in 2015 (16,437 m^3/s) than in 2010 (20,055 m^3/s), showing an 18% depreciation in the flood-discharging capacity of the active river over 5 years.

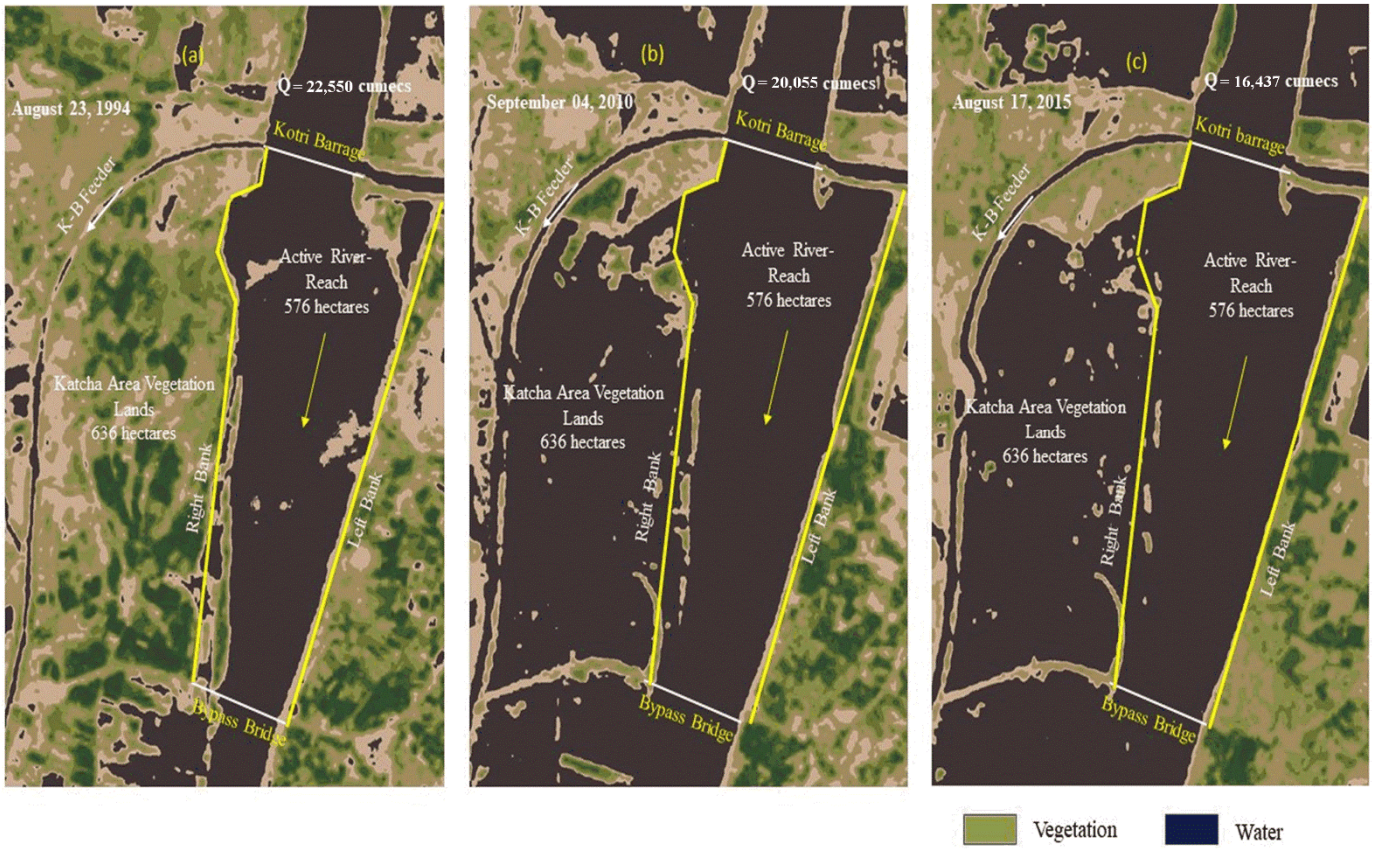

Figure 5. Visual comparisons of Landsat imageries for the study area river-reach. (**a**) TM acquired image on 23 August 1994, passing an exceptionally high flood through active river-reach; (**b**) TM acquired image on 4 September 2010, showing the inundation of Katcha area along with active reach at very high flood; (**c**) OLI and TIRS acquired image on 17 August 2015, depicting the inundation of Katcha area and active river-reach at high flood passing downstream of the Kotri barrage.

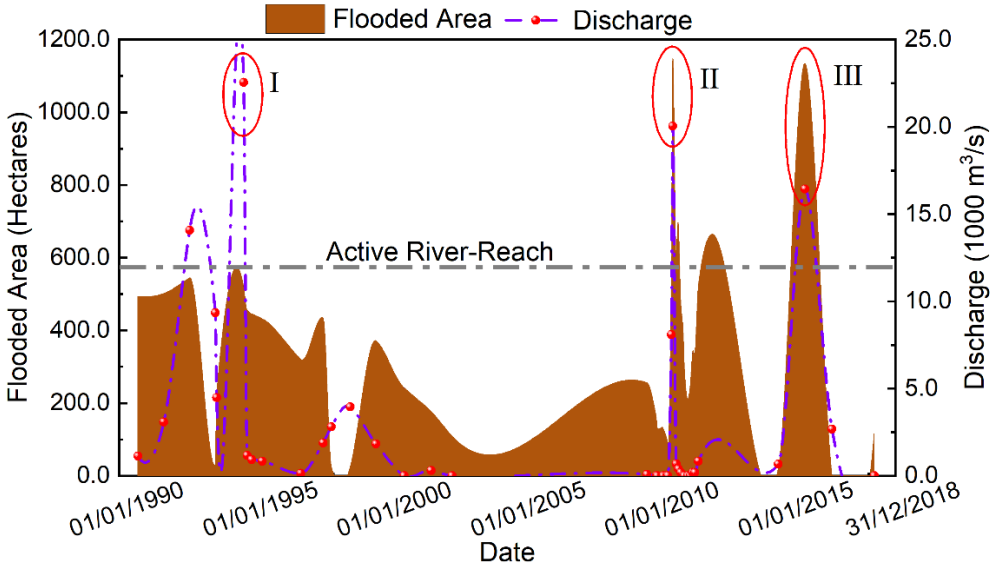

Figure 6. The relation between riverine surface area inundated with water and corresponding discharge: (I) Water-inundated area below active river reach area at exceptionally high flood, i.e., 22,550 m^3/s; (II) Water-inundated area above active river reach area at exceptionally high flood, i.e., 20,055 m^3/s; (III) Water-inundated area exceed active river reach area at high flood, i.e., 16,437 m^3/s.

3.3. Calibration and Validation

Using the installed gauge immediate downstream of the Kotri Barrage, the rating curve (Figure 7) was established for 6 years of data, from 2008 to 2013. Figure 7 illustrates a good relationship between the stage and discharge values, depicting a stable river-reach section. The rating curve was processed for the calibration of the hydraulic model in steady-flow mode (Ackerman, 2009) through comparison of the observed and simulated flow hydrograph for the 2010 flood downstream of the Kotri barrage (Figure 8). The comparison exhibits a good relationship between the simulated and observed hydrographs, as evident from the coefficient of determination (R^2), which is determined to be 0.91. The validation for the calibrated hydraulic model was established using high watermarks on the left bank of the study area river reach. The observed high-water marks for the 2010 flood were compared with simulated watermarks (Figure 9). The root mean square error is 0.184, while the results prove a good correlation between the two, depicting a strong statistical correlation (R^2) of 0.88.

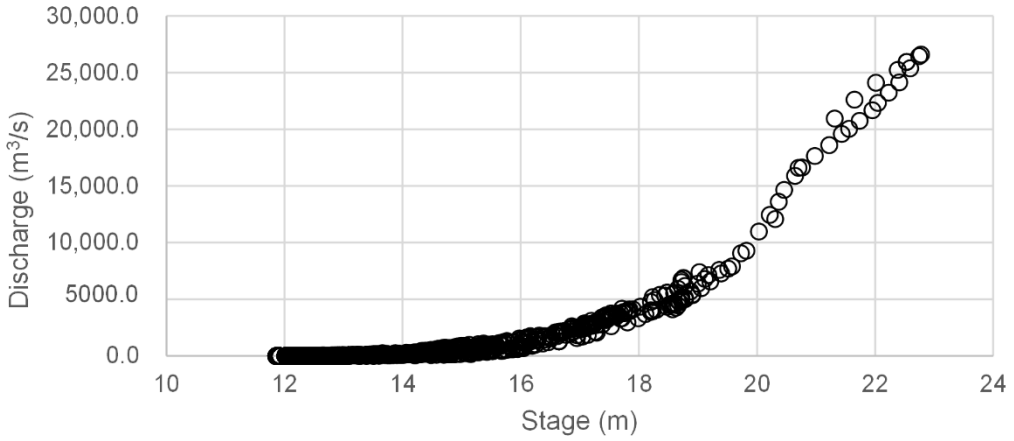

Figure 7. Rating curve based on six-year data from 2008 to 2013 downstream of the Kotri Barrage, Sindh.

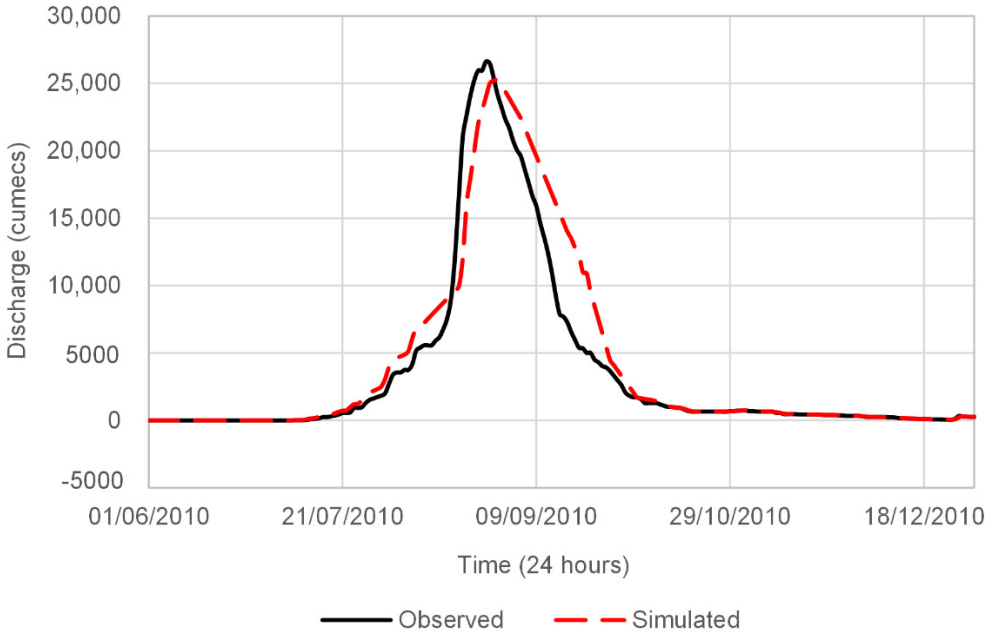

Figure 8. Calibration of the hydraulic model by comparing the observed and simulated flow hydrograph of the 2010 flood downstream of the Kotri Barrage.

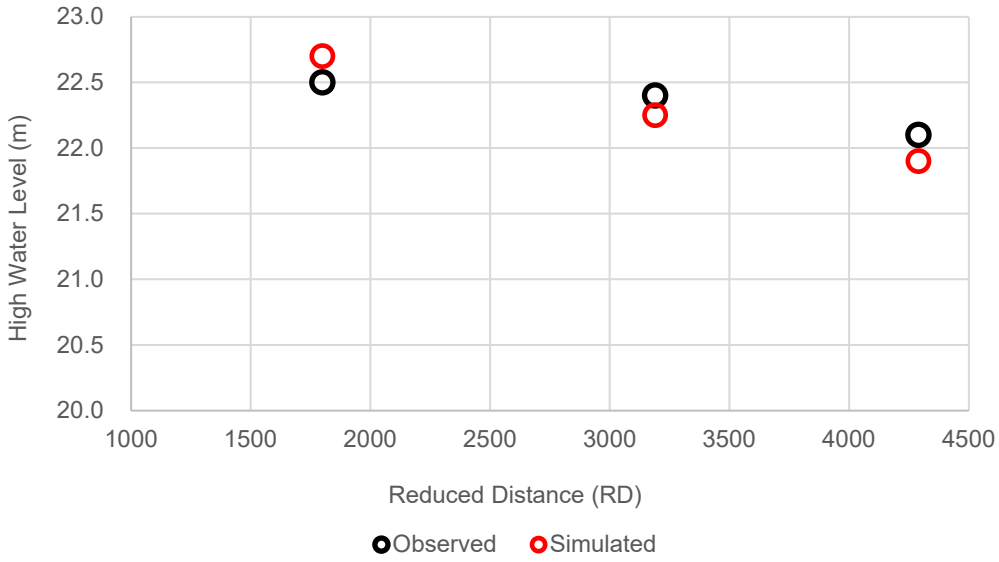

Figure 9. Validation of the hydraulic model by comparing the observed and simulated high water-marks of the 2010 flood downstream of the Kotri Barrage.

3.4. Sediment Deposits Impact Assessment

The scenario-based impact assessment of sediment deposits on the flow regime in the study area river-reach was completed employing the middle braiding cross-sections (Figure 10) for the floodplain system in the HEC-RAS model. It is interpreted coupling remotely sensed imagery and field data of morphologically active channels. Figure 10 compares three middle river-reach x-sections, simulated for the flood years of 1994 and 2010 through an iterative process in the HEC-RAS 1D-unsteady flow analysis model, while observed for the year 2018. They clearly show the vertical profile of the braiding river from three ditch channels in 1994 to two active layers in 2010, and eventually reshaped to one morphologically active channel in 2018. The major contribution in this reshaping is from riverine flows, which have depreciated below the environmental flows downstream of the Kotri barrage.

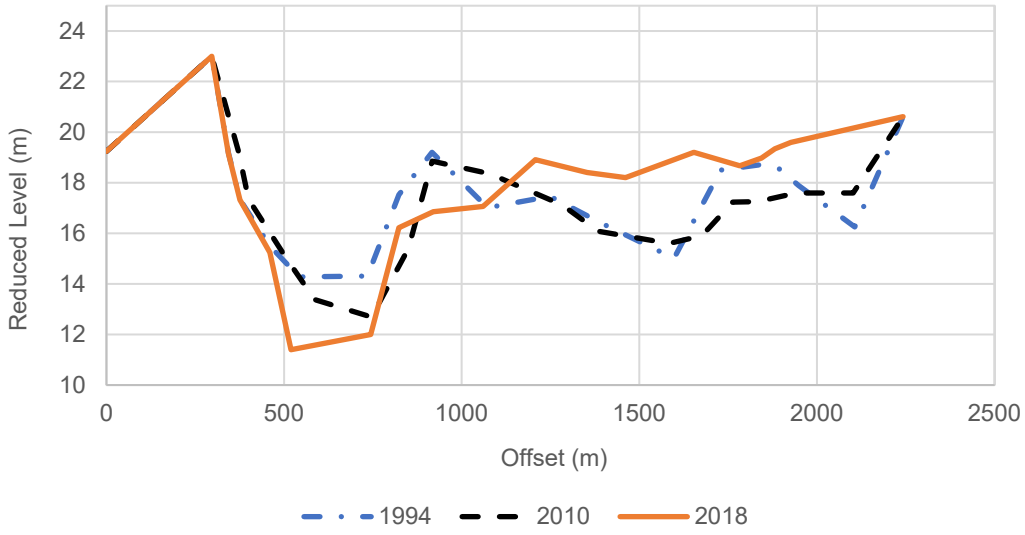

Figure 10. Interpreted cross-sections for the flood year 1994, 2010, and the situation scenario for the year 2018 at the middle river reach.

The flow simulations in the HEC-RAS model have estimated the water surface elevations at the introduced cross-sections of the study area, thus calculating the bank-full discharges and discharges eventuating the levee overflow (Table 3). The 1D-unsteady flow model simulations (Table 3) manifest a 48.34% reduction in the bank-full discharge and a 17.75% reduction in discharge eventuating levee overtop because of a huge chunk of sedimentary deposits on the riverine floodplain. Thus, the alluvium river reaches downstream of the Kotri barrage is morphologically dynamic as it adapts to the changing riverine flow regimes.

Table 3. HEC-RAS 1D-model unsteady flow simulations results for bank-full discharge and discharge eventuating levee overtop.

Hydrologic Year	Bank-Full Discharge (m^3/s)	Discharge Capacity Reduction (%)	Discharge Eventuating Levee Overtop (m^3/s)	Flood Carrying Capacity Reduction (%)
1994	19,850	-	32,480	-
2010	17,600	11.34	31,100	4.25
2018	11,080	37.00	26,900	13.50
Total	-	48.34	-	17.75

3.5. River Geometry Optimization

Various shapes of river geometry cross-sections were assumed and simulated in the HEC-RAS unsteady flow model to establish the ideal cross-section having a maximum discharging capacity potential. The new cross-sectional geometry (Figure 11) idealizes a 100% sediment removal from the river floodplain. Moreover, the 1D-unsteady flow simulations in the HEC-RAS model conclude a 22,954 m^3/s bank-full discharge for the optimized trapezoidal geometry that aftereffect a 51.7% enhancement in flood discharging capacity of the river.

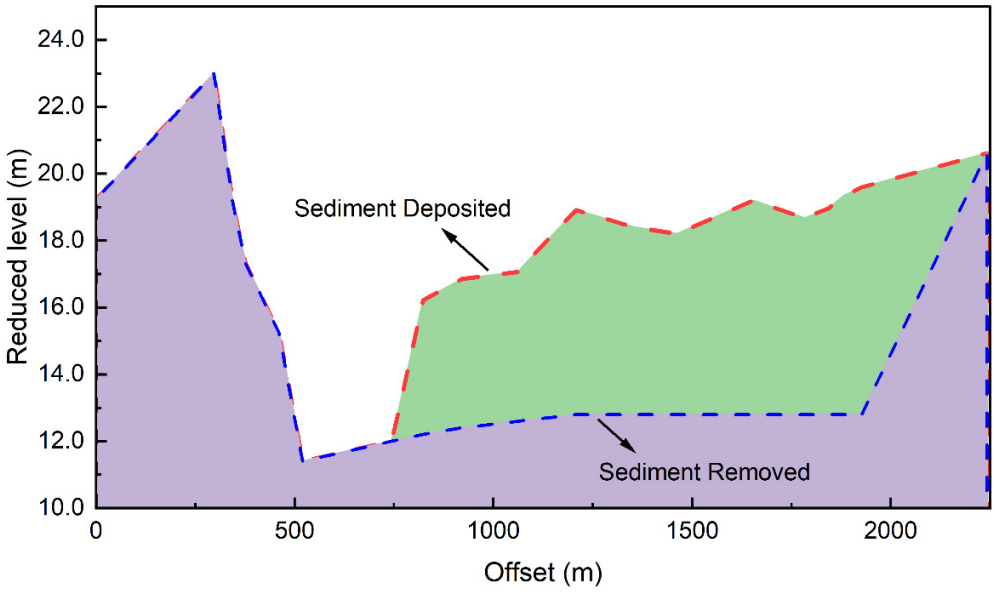

Figure 11. Optimized river geometry for enhancing the flood discharging and flood carrying capacity of the alluvium river-reach.

The volume of the deposited sediments calculated using the ideal and actual cross-section (Figure 11) is 4.3 BCM. Such a high concentration of alluvial deposits and low rates of flow downstream of the Kotri barrage results in the alteration in the configuration of the alluvial bed, to the extent of the difference in the sedimentary movement rate. The immobilization of the bed form and the tightening of the riverine cross-sections pertaining to human interventions, such as hydraulic and flood control structures, implicate high

flood stages, extreme flow velocity, and bank overtopping. The same phenomena occurred to the Lower Yellow River, where the levees breached and avulsion occurred, killing 200,000 people and leaving 7 million homeless [15,34]. Moreover, the sedimentary deposits in the form of dunes can be controlled and scrambled with the Kotri barrage gate operations and the availability of environmental flows, i.e., 5000 m^3/s [19,28] downstream of the Kotri barrage. The September 2022 flooding in the Indus river, pertaining to monsoon, compounded with climate-induced rapid ice melting induced a very high flood, with a flow escapage of 16,990 m^3/s downstream of the Kotri barrage (IRSA). As the flood carrying capacity of the Indus river choked with elevated bed-forms, carrying huge sediment deposits, frequent levee breaches occurred, affecting 33 million people across Pakistan (NDMA) and which compounded the death and destruction to properties and livelihoods. Moreover, these deposits, if removed using engineered or hydrologic means, will result in an 18.5% enhancement in the flood-carrying capacity of the study area river-reach, and the same river training strategy can be employed to enhance the flood-carrying capacity of the Indus river.

4. Conclusions

The philosophy of laterally unstable rivers which possess patterns of river motion and lateral channel deformations due to the aggradation of alluvial deposits on the riverine floodplain is complex and misunderstood. The river pattern is associated with the availability of flows that visualize sediments through degradation and aggradation. The study area river-reach was used as a lab for modeling and understanding the riverine behavior, which responds to the receding flow availability. The laterally unstable behavior of rivers is attributed to a bed elevation increase and the enhancement in flood water extension probability over banks. Such unstable, poorly maintained rivers may result in levee overtopping in the case of a super flood, as is already expected through the changing global climate extremes. Thus, this research may contribute to the survival of obliterated riverine reaches on the verge of flow extinction over elongated periods and in the reduction in flood hazards associated with different flow conditions. This study may be extended as a baseline for further studies to the concept of dominant discharge and its influence on the sediment-flushing mechanism through the development of active river channels in a reach using the erosive power of river flows. It can also help with sediment resource management for the delta ecosystems, which currently face a scarcity of sedimentary deposits.

Author Contributions: Conceptualization, A.M., M.W.I. and A.A.S.; methodology, A.M. and M.W.I.; software, A.M.; validation, M.W.I. and A.A.S.; formal analysis, M.A. and M.Y.; investigation, A.M. and M.W.I.; writing—original draft preparation, A.M. and J.-C.H.; writing—review and editing, A.M., J.-C.H. and A.A.S.; supervision, J.-C.H.; project administration, A.M. and M.A.; funding acquisition, J.-C.H. All authors have read and agreed to the published version of the manuscript.

Funding: This research was funded by the Major Basic Research Development Program of the Science and Technology, Qinghai Province, grant numbers 2021-SF-A6 and 2019-SF-146, the National Natural Science Foundation of China, grant number 51809007, and the Fundamental Research Funds for the Shenzhen University, grant number 2110822.

Data Availability Statement: Not applicable.

Acknowledgments: The authors appreciate the cooperation of Sindh Irrigation Department for provision of access to monitored data and survey in the study area. Additionally, provision of satellite imageries by NASA/USGS and digital elevation model by the Japan Aerospace Exploration Agency, free of charges, is also acknowledged.

Conflicts of Interest: The authors declare no conflict of interest.

References

1. Ashmore, P.; Peirce, S.; Leduc, P. Expanding the "Active Layer": Discussion of Church and Haschenburger (2017) What is the "Active Layer"? *Water Resour. Res.* **2018**, *54*, 1425–1427. [CrossRef]
2. Leduc, P.; Ashmore, P.; Gardner, T. Grain sorting in the morphological active layer of a braided river physical model. *Earth Surf. Dyn. Discuss.* **2015**, *3*, 577–600. [CrossRef]
3. Ashmore, P.; Bertoldi, W.; Tobias Gardner, J. Active width of gravel-bed braided rivers. *Earth Surf. Process. Landforms* **2011**, *36*, 1510–1521. [CrossRef]
4. Alekseevskiy, N.I.; Berkovich, K.M.; Chalov, R.S. Erosion, sediment transportation and accumulation in rivers. *Int. J. Sediment Res.* **2008**, *23*, 93–105. [CrossRef]
5. Ali, A. *Indus Basin Floods: Mechanisms, Impacts and Management*; Asian Development Bank: Mandaluyong, Philippines, 2013.
6. Agro-Dev, A. Tarbela dam and related aspects of the Indus river basin systems. In *WCD Case Study*; International (Pvt.) Ltd.: Islamabad, Pakistan, 2000.
7. Inam, A.; Khan, T.; Tabrez, A.; Amjad, S.; Danish, M.; Tabrez, S. *Natural and Man Made Stresses on the Stability of Indus Deltatic Eco-Region*; Geolo: Bangkok, Thailand, 2003.
8. Giosan, L.; Constantinescu, S.; Clift, P.D.; Tabrez, A.R.; Danish, M.; Inam, A. Recent morphodynamics of the Indus delta shore and shelf. *Cont. Shelf Res.* **2006**, *26*, 1668–1684. [CrossRef]
9. Jorgensen, D.W.; Harvey, M.D.; Schumm, S.A.; Flam, L. *Morphology and Dynamics of the Indus River: Implications for the Mohen jo Daro Site*; Himalaya to the Sea; Shroder, J.F.J., Ed.; Routledge: London, UK, 1993; pp. 228–326.
10. Vörösmarty, C.J.; Meybeck, M.; Fekete, B.; Sharma, K.; Green, P.; Syvitski, J.P.M. Anthropogenic sediment retention: Major global impact from registered river impoundments. *Glob. Planet. Chang.* **2003**, *39*, 169–190. [CrossRef]
11. Syvitski, J.P.M.; Vörösmarty, C.J.; Kettner, A.J.; Green, P. Impact of Humans on the Flux of Terrestrial Sediment to the Global Coastal Ocean. *Science* **2005**, *308*, 376–380. [CrossRef]
12. Ali, K.F.; De Boer, D.H. Spatial patterns and variation of suspended sediment yield in the upper Indus River basin, northern Pakistan. *J. Hydrol.* **2007**, *334*, 368–387. [CrossRef]
13. Holmes, D.A. The Recent History of the Indus. *Geogr. J.* **1968**, *134*, 367. [CrossRef]
14. West Pakistan Water and Power Development Authority. *Indus River Flow Data into Reservoir of Pakistan*; West Pakistan Water and Power Development Authority: Lahore, Pakistan, 2017.
15. Wang, Z.Y.; Lee, J.H.; Melching, C.S. Estuary Processes and Management. In *River Dynamics and Integrated River Management*; Springer: Berlin, Germany, 2015; pp. 467–554.
16. Guo, L.; Su, N.; Zhu, C.; He, Q. How have the river discharges and sediment loads changed in the Changjiang River basin downstream of the Three Gorges Dam? *J. Hydrol.* **2018**, *560*, 259–274. [CrossRef]
17. West Pakistan Water and Power Development Authority. *Lower Indus Report, The Atlas*; West Pakistan Water and Power Development Authority: Lahore, Pakistan, 1965.
18. Boota, M.W.; Yan, C.; Idrees, M.B.; Li, Z.; Dou, M.; Zohaib, M.; Yousaf, A. Assessment of the morphological trends and sediment dynamics in the Indus River, Pakistan. *J. Water Clim. Chang.* **2021**, *12*, 3082–3098. [CrossRef]
19. Ijaz, M.W.; Mahar, R.B.; Ansari, K.; Siyal, A.A.; Anjum, M.N. Integrated assessment of contemporary hydro-geomorphologic evolution of the Indus River Estuary, Pakistan in context to regulated fluvial regimes. *Estuar. Coast. Shelf Sci.* **2020**, *236*, 106657. [CrossRef]
20. Singh, M.; Singh, I.B.; Müller, G. Sediment characteristics and transportation dynamics of the Ganga River. *Geomorphology* **2007**, *86*, 144–175. [CrossRef]
21. Lu, H.; Burbank, D.W.; Li, Y.; Liu, Y. Late Cenozoic structural and stratigraphic evolution of the northern Chinese Tian Shan foreland. *Basin Res.* **2010**, *22*, 249–269. [CrossRef]
22. Nepal, S.; Shrestha, A.B. Impact of climate change on the hydrological regime of the Indus, Ganges and Brahmaputra river basins: A review of the literature. *Int. J. Water Resour. Dev.* **2015**, *31*, 201–218. [CrossRef]
23. Rasul, G.; Mahmood, A.; Sadiq, A.; Khan, S. Vulnerability of the Indus Delta to Climate Change in Pakistan. *Pak. J. Meteorol.* **2012**, *8*, 89–107.
24. Cruff, R.W.; Rantz, S.E. *A Comparison of Methods Used in Flood-Frequency Studies for Coastal Basins in California*; U.S. Government Printing Office: Washington, DC, USA, 1965.
25. Dalrymple, T. *Flood-Frequency Analyses, Manual of Hydrology: Part 3*; 1543-A; U.S. Government Publishing Office: Washington, DC, USA, 1960.
26. McFeeters, S.K. The use of the Normalized Difference Water Index (NDWI) in the delineation of open water features. *Int. J. Remote Sens.* **1996**, *17*, 1425–1432. [CrossRef]
27. Yang, B.; Tong, S.T.Y.; Fan, R. Using High Resolution Images from UAV and Satellite Remote Sensing for Best Management Practice Analyses. *J. Environ. Inform.* **2021**, *37*, 79–92. [CrossRef]
28. Ijaz, M.W.; Siyal, A.A.; Mahar, R.B.; Ahmed, W.; Anjum, M.N. Detection of Hydromorphologic Characteristics of Indus River Estuary, Pakistan, Using Satellite and Field Data. *Arab. J. Sci. Eng.* **2017**, *42*, 2539–2558. [CrossRef]
29. Tadono, T.; Ishida, H.; Oda, F.; Naito, S.; Minakawa, K.; Iwamoto, H. Precise Global DEM Generation by ALOS PRISM. *ISPRS Ann. Photogramm. Remote Sens. Spat. Inf. Sci.* **2014**, *II-4*, 71–76. [CrossRef]

30. Ijaz, M.W.; Mahar, R.B.; Ansari, K.; Siyal, A.A. Optimization of salinity intrusion control through freshwater and tidal inlet modifications for the Indus River Estuary. *Estuar. Coast. Shelf Sci.* **2019**, *224*, 51–61. [CrossRef]
31. Brunner, G.W. *HEC-RAS River Analysis System. Hydraulic Reference Manual. Version 4.1*; U.S. Army Corps of Engineers, Hydrologic Engineering Center: Davis, CA, USA, 2010.
32. Chow, V.T. *Open Channel Hydraulics*; McGraw-Hill Co.: New York, NY, USA, 1959.
33. Simons, Li & Associates, Inc. *Design Manual for Engineering Analysis of Fluvial Systems*; Arizona Department of Water Resources: Phoenix, AZ, USA, 1985.
34. Hu, Y.M.; Liang, Z.M.; Solomatine, D.P.; Wang, H.M.; Liu, T. Assessing the Impact of Precipitation Change on Design Annual Runoff in the Headwater Region of Yellow River, China. *J. Environ. Inform.* **2021**, *37*, 122–129. [CrossRef]